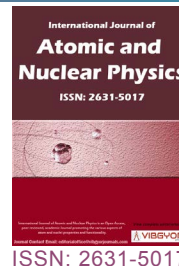


Coincidence Summing Correction for Cylinder and Marinelli Beaker Sources by Monte Carlo Simulation



Waseem Khan, Chaohui He* and Yu Cao

Department of Nuclear Science and Technology, Xi'an Jiaotong University, China

Abstract

Coincidence summing effects arises when two or more γ -rays are emitted in a cascade from an excited nucleus and are detected within the resolving time of the detector. Without correction of such effects, the activity of radionuclides cannot be accurately determined. For the correction of summing effects, a new simulation method in GEANT4 was established to simulate the coincidence summing correction factors (CSF_{simu}) for an HPGe detector. In the simulation, a cylindrical and Marinelli beaker source containing several radionuclides were used with different volumes, covering the energy range from 59.50 keV to 1836.01 keV. In the case of volumetric sources, the coincidence summing correction factors for two nuclides (^{60}Co and ^{88}Y) were calculated from the efficiencies at different points throughout the source volume. The dependence of the coincidence correction factor on the sample density was also carried out for some particular nuclide and photon energy. The same methodology of coincidence summing correction factor was applied for the complex decay scheme of ^{133}Ba and ^{152}Eu obtained a good agreement with the experimental results.

Keywords

GEANT4, HPGe detector, Coincidence summing, Marinelli beaker sources

Introduction

γ -ray spectrometry with HPGe detector is widely used to determine the activity of radionuclides in environmental samples. The accurate assessment of the activity of radionuclides would require a minimum source-detector distance to reduce the detection limit of the measuring system. The coincidence summing effect is more significant at a small source-detector distance because the probability of two γ -rays reaching the detector at the same time cannot be negligible at such distance.

The coincidence summing effect changes in the count from the peaks corresponding to the two γ -rays and nuclides activity become inaccurate if no correction is performed. For the correction of such effects, the contribution of total efficiency is also required with the full energy peak efficiency. Various groups used different calibration techniques and obtained the coincidence summing correction factors (CSFs) from the total efficiency. Debertin & Schötzig [1] used the experimental technique and calculated the CSF from the total efficiency (the ratio of the total number of pulses recorded to the

*Corresponding author: Chaohui He, Department of Nuclear Science and Technology, School of Energy and Power Engineering, Xi'an Jiaotong University, Xi'an 710049, China

Accepted: May 18, 2019; Published: May 20, 2019

Copyright: © 2019 Khan W, et al. This is an open-access article distributed under the terms of the Creative Commons Attribution License, which permits unrestricted use, distribution, and reproduction in any medium, provided the original author and source are credited.

Khan et al. *Int J At Nucl Phys* 2019, 4:011

ISSN 2631-5017



9 772631 501003

Citation: Khan W, He C, Cao Y (2019) Coincidence Summing Correction for Cylinder and Marinelli Beaker Sources by Monte Carlo Simulation. *Int J At Nucl Phys* 4:011

number of photons emitted by the source). Practically, the total efficiency curve is difficult to achieve due to the single γ -ray emitting nuclides and preparation of standard sources. Several authors used the analytical approaches for the calculation of the CSF from the total efficiency [2-9]. These approaches required information about the nuclear decay parameters such as the mode of parent nuclide decay, conversion factors, and the probability for the γ -ray transition from one energy level to another etc. Z Wang, et al. [10] used the Monte Carlo code MCNP and simulated the total efficiencies for the correction of coincidence summing effect. They used point source to test the coincidence summing correction method and observed a coincidence peak efficiency of at small source-detector distances. However such analysis is difficult to achieve for the close geometry measurements and large volume samples because in volumetric sources the contribution of the scattered γ -rays to the total efficiency cannot be neglected [11]. Many authors proposed an approach of point sources positioned in the matrix of the extended source for the calculation of peak, total efficiencies and CSF [4,12-15]. Tk Wang, et al. [4] include the effects of volume factor in the CSF values and observed a good agreement between calculated and experimental results. Recent techniques [16,17] in GEANT4 were good for the calculation of CSF, but such computational techniques required elaborate work in its implementation.

The aim of this paper is to develop a simplest and modest method in Geant4 for the coincidence summing correction factors (CSF_{simu}) of the extended sources. The CSF_{simu} values were compared with the calculated and experimental results reported by Wang, et al. [4] and obtained good agreements.

Materials and Methods

GEANT4 [18] toolkit includes simulation of the electromagnetic interaction of charged particle, gamma, and optical photons. The code follows the history of each individual primary photon until its energy dissipated in the detector and produces secondary particles as a result of photoelectric effect, Compton effect, pair production interaction, multiple scattering, bremsstrahlung, and ionization. The secondary electrons formed by photon interaction processes were also taken into consideration in the simulation. GEANT4 electromagnetic physics class was used in the simulation since the energy limit for the electromagnetic process is 10 keV to 100 TeV. Therefore, Ge X-rays of energy below 10 keV cannot be processed. GEANT4 also includes low-level electromagnetic processes that can simulate a particle down to 250 eV. The number of total histories (10^7 primary photons) was considered for the simulation to obtain a statistical uncertainty of no more than 0.1%. All the photon energies emitted by the source were individually simulated for the source-detector geometries.

Only the γ -rays, which deposit their full energy

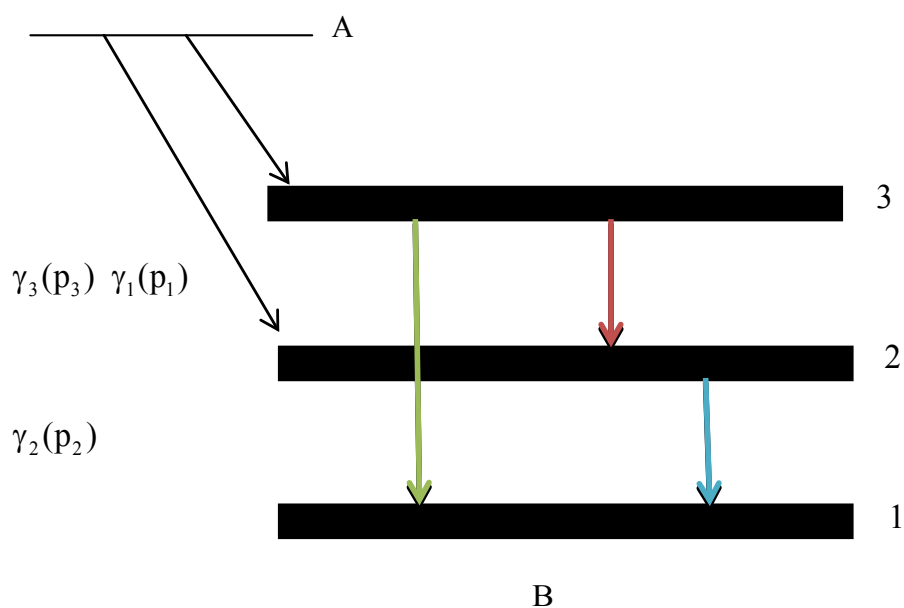


Figure 1: A typical decay scheme to show the coincidence summing effect.

in the active volume of the detector, were considered for the evaluation of full energy peak efficiency. The simulated full energy peak efficiencies are obtained from

$$\varepsilon = \frac{Q}{M} \tag{1}$$

where ε is the full energy peak efficiency, Q is the number of counts that deposit their full energy in the active detector volume, and M is the number of total simulated γ -rays counts for a given energy, E .

In order to simulate the total efficiencies and CSFs, a detailed decay scheme is considered as shown in Figure 1. The nuclide A decays to the two excited states of B . The two excited states deexcite by the emission of three γ -rays γ_1 ($3 \rightarrow 2$), γ_2 ($2 \rightarrow 1$), γ_3 ($3 \rightarrow 1$) with their respective probabilities as P_1 , P_2 , and P_3 .

In absence of coincidence summing, the count rate is given by;

$$N_1 = A p_1 \varepsilon_1 \tag{2}$$

Where A is the source activity, p_1 is the emission probability with energy E_1 and ε_1 is peak efficiency for γ_1 with E_1 .

The count rate N_1^* in the recorded full energy peak will be smaller than N_1 . So the in presence of coincidence summing the count rate is given by

$$N_1^* = A p_1 \varepsilon_1 - A p_1 \varepsilon_1 \varepsilon_{T2} \tag{3}$$

Where ε_{T2} is the total detection efficiency for γ_2 . The CSF_{Simu} for γ_1 is given by

$$\frac{N_1}{N_1^*} = \frac{1}{1 - \varepsilon_{T2}} \tag{4}$$

$$\frac{N_1^*}{N_1} = 1 - \varepsilon_{T2} \tag{5}$$

$$CSF_{Simu}^a = 1 - \varepsilon_{Tsimu}^b \tag{6}$$

Similarly for γ_2 ,

$$N_2 = A p_2 \varepsilon_2 \tag{7}$$

$$N_2^* = A p_2 \varepsilon_2 - A p_1 \varepsilon_2 \varepsilon_{T1} \tag{8}$$

$$\frac{N_2}{N_2^*} = \frac{1}{1 - \frac{p_1}{p_2} \varepsilon_{T1}} \tag{9}$$

$$\frac{N_2^*}{N_2} = 1 - \frac{p_1}{p_2} \varepsilon_{T1} \tag{10}$$

Or

$$CSF_{Simu}^b = 1 - \frac{p_1}{p_2} \varepsilon_{Tsimu}^a \tag{11}$$

Where CSF_{Simu}^a and CSF_{Simu}^b are the simulated coincidence summing correction factors, ε_{Tsimu}^a and ε_{Tsimu}^b are the simulated total efficiencies of 1173.24 keV (a) and 1332.50 keV (b) respectively, similarly for ^{88}Y , ^{133}Ba and ^{152}Eu .

The coincidence summing effects become more complicated for the extended volume sources. In this case, the correction factor not only depends on the peak and total efficiencies but also on the source volume and the differential efficiency distributions within the source. For volume sources, the CSF_{Simu} is given by

$$CSF_{Simu}^a = \frac{\int \rho \varepsilon_1 (1 - \varepsilon_{Tsimu}^b) d\rho}{\int \rho \varepsilon_1 d\rho} \tag{12}$$

$$CSF_{Simu}^b = \frac{\int \rho \varepsilon_2 \left(1 - \frac{p_1}{p_2} \varepsilon_{Tsimu}^a\right) d\rho}{\int \rho \varepsilon_2 d\rho} \tag{13}$$

Or, as a summation,

$$CSF_{Simu}^a = 1 - \left[\frac{\sum \rho_i \varepsilon_1 \varepsilon_{Tsimu}^b d\rho}{\sum \rho_i \varepsilon_1 d\rho} \right] \tag{14}$$

$$CSF_{Simu}^b = 1 - \left[\frac{\sum \rho_i \varepsilon_2 \frac{p_1}{p_2} \varepsilon_{Tsimu}^a d\rho}{\sum \rho_i \varepsilon_2 d\rho} \right] \tag{15}$$

Where ρ_i are the radial positions of the point sources from the beaker axis. Eq 14 and Eq 15 can be written as

$$CSF_{Simu}^a = 1 - \langle J_1 \rangle \tag{16}$$

For h_1 ,

$$J_{1h_1} = \frac{\sum \rho_i \varepsilon_1 \varepsilon_{Tsimu}^b d\rho}{\sum \rho_i \varepsilon_1 d\rho} \tag{17}$$

For the whole volume source height,

$$\langle J_1 \rangle = \frac{\sum_{i=1}^3 J_{1h_i}}{3} \tag{18}$$

Where h_i are the different distances from the beaker bottom. Similarly,

$$CSF_{Simu}^b = 1 - \langle J_2 \rangle \tag{19}$$

$$J_{2h_1} = \frac{\sum \rho_i \varepsilon_2 \varepsilon_{Tsimu}^a d\rho}{\sum \rho_i \varepsilon_2 d\rho} \tag{20}$$

$$\langle J_2 \rangle = \frac{\sum_{i=1}^3 J_{2h_i}}{3} \tag{21}$$

Where $\langle J_1 \rangle$ and $\langle J_2 \rangle$ are the average of 15-point integration of efficiencies.

To calculate the coincidence summing correction for all volumes, first, the cylinder and Marinelli beaker volumes are divided into three volumes (h_1 , h_2 , and h_3) and then further subdivided into 5 volume elements J_{1h_i} for each (h_1 , h_2 , and h_3). Every single nuclide in ^{60}Co , ^{88}Y , and ^{152}Eu considered as a point source with their respective photon energies and placed at 15 positions within the source volume with three different distances (h_1 , h_2 , and h_3) from the beaker bottom. To get J_{1h} for 898.02 keV or 1173.24 keV at volume source height h_1 , first computed the ϵ and $\epsilon_{\text{Tsimu}}^b$ (at 1836.01 keV or 1332.50 keV) values at 5 different positions in the source volume and then computed the 5-point integration (i.e., multiplied each value by ρ_i , summed them, and divided by the sum of the $\rho_i \epsilon$). Similarly, calculated J_{1h_2} (5-point integration of efficien-

cies) and J_{1h_3} (5-point integration of efficiencies) at height h_2 and h_3 respectively and averaged them to get $\langle J_1 \rangle$ at 15 volume elements except for the axial position of the beaker. The ϵ and ϵ_{Tsimu} value does not change with the further subdivision of the beaker volume. The same method was applied for 1836.01 keV and 1332.50 keV to obtain $\langle J_2 \rangle$ but used $\epsilon_{\text{Tsimu}}^a$ (898.02 keV and 1173.24 keV) respectively in this case. The CSF values were also obtained for ^{133}Ba (276.39 keV, 302.85 keV) and ^{152}Eu (778.9 KeV, 964.0 keV and 444.0 KeV) nuclides using the same procedures.

The detector considered for MC simulation was a p-type coaxial HPGe detector (Canberra). The main parameters of the detector provided by the manufacturer are shown in Figure 2. No information was available by the manufacturer about whether the Ge crystals had rounded edges. Sharp edges of the crystals were assumed in the simulation. First, a cylindrical beaker source of diameter ($D = 43.4$ mm) filled with gamma radionuclides aqueous solution of volumes V1 (50 mL), V2 (100 mL), V3 (200 mL), and V4 (300 mL) was used to obtain the values. A Marinelli

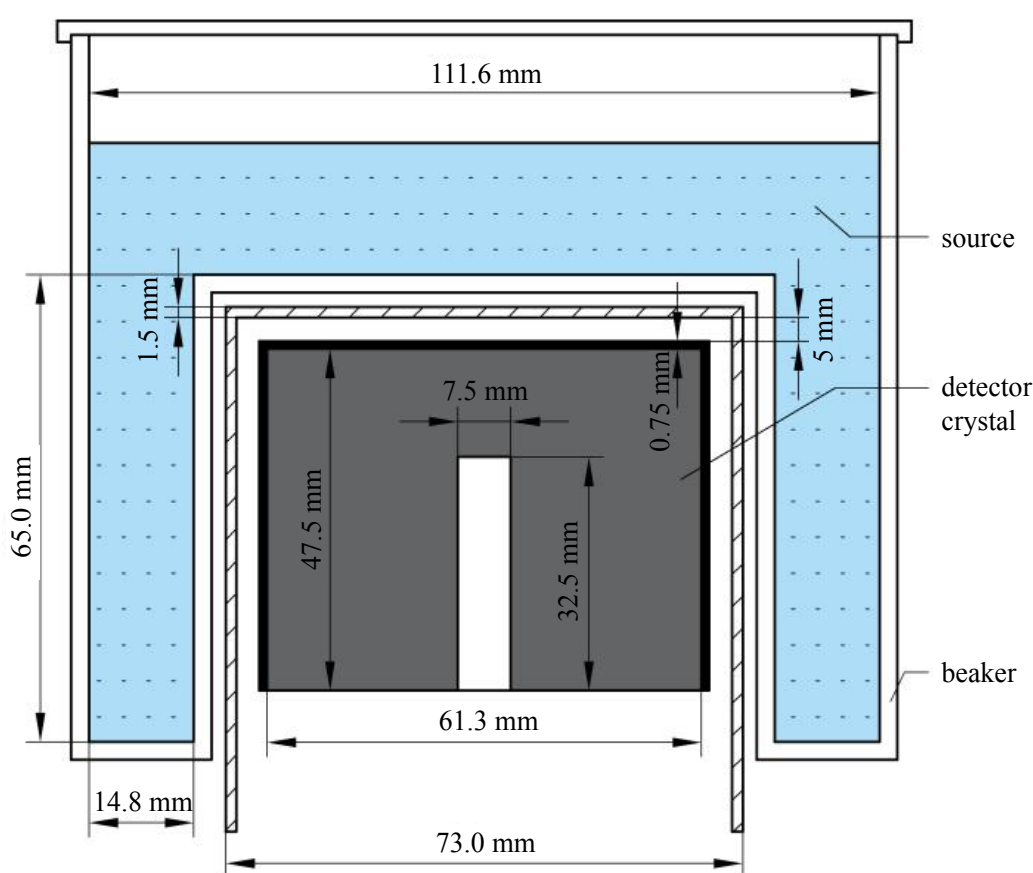


Figure 2: Schematic of the detector with Marinelli beaker source.

Table 1: Single line and multi gamma ray nuclides with emission probability.

Nuclide	Energy (keV)	P(%)
²⁴¹ Am	59.50	
¹⁰⁹ Cd	88.02	
⁶⁵ Zn	111.50	
⁵⁷ Co	122.06	
¹⁴¹ Ce	145.44	
¹³⁹ Ce	165.85	
⁵¹ Cr	320.08	
¹¹³ Sn	391.69	
¹³⁷ Cs	661.66	
⁵⁴ Mn	834.84	
⁸⁸ Y	898.02	93.70
	1836.01	99.35
⁶⁰ Co	1173.24	99.90
	1332.50	99.98
¹³³ Ba	276.39	7.164
	160.61	0.645
	302.85	18.33 34.06
	80.99	
¹⁵² Eu	778.9	13.06 26.78
	344.3	2.79
	444.0	10.12
	1085.9	14.5
	964.0	28.81
	121.8	

beaker source whose dimension is shown in Figure 2 with volumes V5 (450 mL), V6 (600 mL), V7 (800 mL) and V8 (1000 mL) was also used in the simulation. The cylinder beaker source was placed at a distance of 6.5 mm while the Marinelli beaker was placed in contact with the detector end-cap window. The radionuclides contained in the source solution with the γ -ray emission probability (P) are listed in Table 1. These nuclides were placed within the cylinder volumes at positions ($h_1 = 1.6$ mm, $h_2 = 2.6$ mm and $h_3 = 3.6$ mm) and ρ_i (5.32 mm, 16.5 mm, 25.5 mm, 34.5 mm and 42.5 mm) and Marinelli beaker volumes at ($h_1 = 30$ mm, $h_2 = 60$ mm and $h_3 = 90$ mm) and (22 mm, 44 mm, 66 mm, 88 mm and 110 mm).

Results and Discussion

In order to simulate the CSF, the total efficiency

is always required with the full energy peak efficiency. The simulated full energy peak and total efficiency curves for cylindrical and Marinelli beaker sources with different volumes are shown in Figure 3 and Figure 4. The figures show that the full energy peak and total efficiency increases for the various volumes with the photon energy around 122.06 keV where the maximum values for the full energy peak and total efficiency were obtained. The full energy peak and total efficiency are close to each other at the low energy range because the absorption of the γ -rays in a single photoelectric interaction is predominated only for energies below about 145.44 keV as shown in figures. At high photon energy, the full energy peak efficiency drops off faster than the total efficiency because of the probability of Compton scattering followed by photoelectric absorption of the scattered photon is dominant than the absorption of the full photon energy in a single photoelectric event. As shown in figures the multiple scattering is the dominant contributor to the total efficiency over all but the lowest range of γ -ray energies. The total efficiency drops off slowly with the increased photon energy due to the less probability of scattered photon in the crystal active volume.

The 15-point integration of efficiency ($\langle J \rangle$) values obtained with our simulation approach is simple and precise to be used to calculate the CSF. The $\langle J \rangle$ values of the nuclides ⁶⁰Co and ⁸⁸Y for the various source volumes are listed in Table 2. The $\langle J \rangle$ values for each source volumes are smaller at low energies and significantly increase at high energy range as shown in Table 2. The computed $\langle J \rangle$ value depends on the source volumes. In volumes (50-300 ml) and (450-1000 ml), the $\langle J \rangle$ values decrease with the increase of source volumes for each photon energy. For Marinelli beaker source the $\langle J \rangle$ value is greater because of the close contact and the small distance of the source inside in the Marinelli beaker to the detector is shown in Table 2.

The CSF values were simulated for cylindrical and Marinelli beaker sources filled with aqueous solution of density 1 g/cm³. The values of the simulated coincidence summing correction factor (CSF_{simu}) obtained from Eq. 16 and Eq. 19 for (⁶⁰Co and ⁸⁸Y) are shown in Table 3 and Table 4. The CSF_{simu} is independent of the detector count rate but it is strongly dependent on the full energy peak and total efficiency. The CSF_{simu} values were

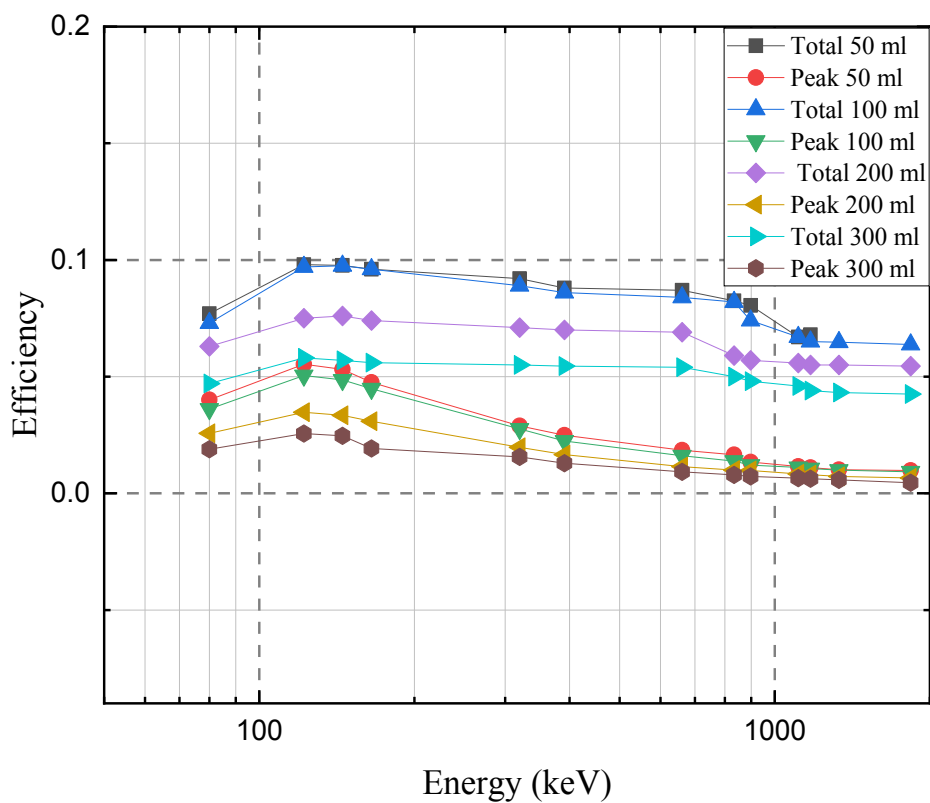


Figure 3: Simulated peak and total efficiencies for cylindrical beaker source.

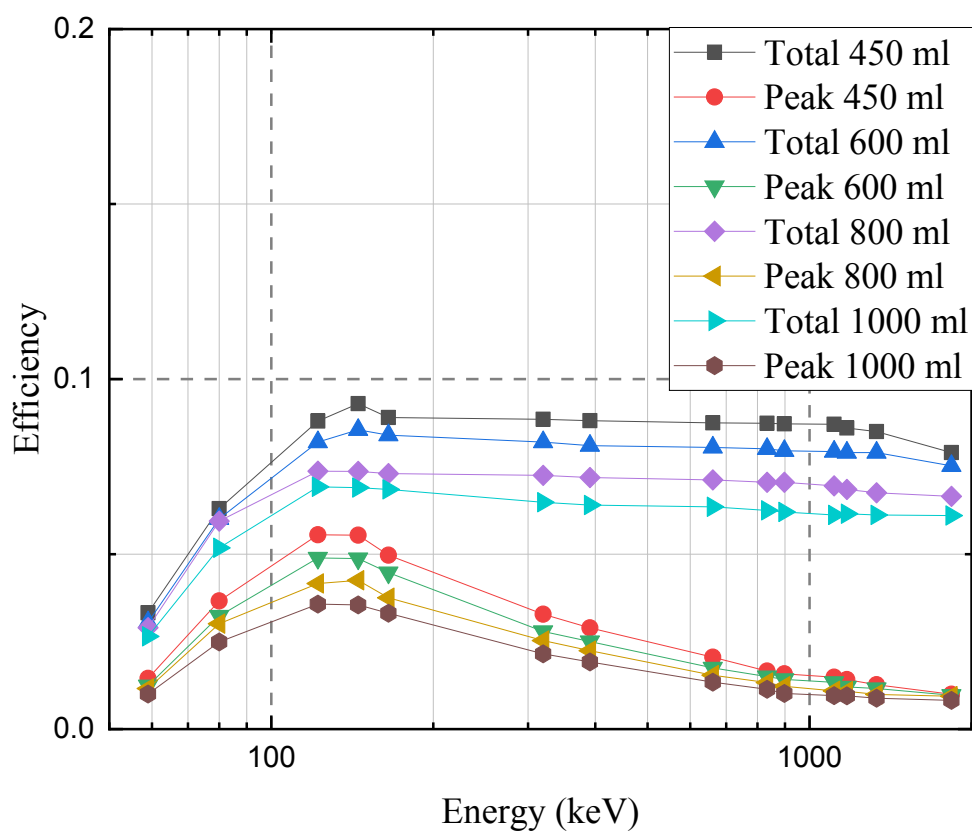


Figure 4: Simulated peak and total efficiencies for Marinelli beaker source.

Table 2: Computed 15-point integration of efficiency values for cylindrical and Marinelli beaker sources.

Energy (keV)	15-point integration of efficiencies	Volume (ml)		Volume (ml)	
1173.24	$\langle J_1 \rangle$	50	0.076	450	0.120
1332.50	$\langle J_1 \rangle$		0.078		0.133
898.02	$\langle J_1 \rangle$		0.043		0.091
1836.01	$\langle J_2 \rangle$		0.099		0.153
1173.24	$\langle J_1 \rangle$	100	0.074	600	0.118
1332.50	$\langle J_2 \rangle$		0.075		0.129
898.02	$\langle J_1 \rangle$		0.049		0.099
1836.01	$\langle J_2 \rangle$		0.108		0.169
1173.24	$\langle J_1 \rangle$	200	0.073	800	0.114
1332.50	$\langle J_2 \rangle$		0.075		0.125
898.02	$\langle J_1 \rangle$		0.058		0.104
1836.01	$\langle J_2 \rangle$		0.120		0.176
1173.24	$\langle J_1 \rangle$	300	0.072	1000	0.111
1332.50	$\langle J_2 \rangle$		0.074		0.109
898.02	$\langle J_1 \rangle$		0.062		0.107
1836.01	$\langle J_2 \rangle$		0.128		0.188

Table 3: Comparison between experimental and simulated coincidence summing correction factors for the cylindrical source.

Volume (ml)	Energy (keV)	CSF _{Exp}	CSF _{Cal}	CSF _{Simu}	RD (%)
50	1173.24	0.917	0.923	0.924	-0.7
	1332.50	0.916	0.921	0.922	-0.6
	898.02			0.957	
	1836.01			0.901	
100	1173.24	0.921	0.927	0.926	-0.5
	1332.50	0.905	0.925	0.925	-2.1
	898.02			0.951	
	1836.01			0.892	
200	1173.24	0.923	0.935	0.927	-0.4
	1332.50	0.911	0.934	0.925	-1.5
	898.02			0.942	
	1836.01			0.880	
300	1173.24	0.922	0.938	0.928	-0.6
	1332.50	0.905	0.937	0.926	-2.2
	898.02			0.938	
	1836.01			0.872	

compared with the experimental and calculated results and obtained good agreement with the relative deviation equal to 2%. For each multi γ -ray

nuclide, the CSF_{simu} value is somewhat greater at low photon energy because of the greater $\langle J \rangle$ value at high photon energy, which means that there is an

Table 4: Comparison between experimental and simulated coincidence summing correction factors for Marinelli beaker source.

Volume (ml)	Energy (keV)	CSF _{Exp}	CSF _{Cal}	CSF _{Simu}	RD (%)
450	1173.24	0.875	0.901	0.880	-0.5
	1332.50	0.858	0.900	0.867	-0.1
	898.02			0.909	
	1836.01			0.847	
600	1173.24	0.874	0.906	0.882	-0.9
	1332.50	0.867	0.905	0.871	-0.4
	898.02			0.901	
	1836.01			0.831	
800	1173.24	0.872	0.909	0.886	-1.6
	1332.50	0.868	0.908	0.875	-0.8
	898.02			0.896	
	1836.01			0.824	
1000	1173.24	0.884	0.911	0.889	-0.5
	1332.50	0.877	0.910	0.891	-1.5
	898.02			0.893	
	1836.01			0.812	

Table 5: Comparison of the simulated coincidence summing correction factors for different densities.

Volume (ml)	Energy (keV)	CSF _{Simu}	Density	ρ (g/cm ³)
50	1173.24	0.920	0.924	0.945
	1332.50	0.916	0.922	0.945
100	1173.24	0.922	0.926	0.950
	1332.50	0.917	0.925	0.947
200	1173.24	0.923	0.927	0.962
	1332.50	0.917	0.925	0.962
300	1173.24	0.924	0.928	0.971
	1332.50	0.920	0.926	0.970
450	1173.24	0.859	0.880	0.931
	1332.50	0.832	0.867	0.929
600	1173.24	0.828	0.882	0.937
	1332.50	0.822	0.871	0.936
800	1173.24	0.810	0.886	0.948
	1332.50	0.801	0.875	0.946
1000	1173.24	0.781	0.889	0.957
	1332.50	0.772	0.891	0.956

inverse relationship between $\langle J \rangle$ and CSF_{simu} values.

To observe the sample density effect on the CSF_{simu} value, the simulation was performed for ethanol, water and sea sand sample (major component SiO₂) with densities (0.7, 1 and 2.5 g/cm³) respec-

tively. The comparison of the CSF_{simu} values for cylindrical and Marinelli beaker sources with different sample density are shown in Table 5. When the density of sample increases the CSF_{simu} value increases because the minimum number of γ -rays

Table 6: Comparison of experimental and simulated coincidence summing correction factors of ^{133}Ba for cylindrical source.

Volumes (ml)	Energy (keV)	CSF _{Exp}	CSF _{Cal}	$\langle J_1 \rangle \langle J_2 \rangle$	CSF _{Simu}	RD (%)
50	276.39	0.915	0.924	0.062	0.938	-2.5
	302.85	0.937	0.959	0.033	0.967	-3.2
100	276.39	0.934	0.925	0.069	0.931	0.3
	302.85	0.944	0.959	0.042	0.958	-1.4
200	276.39	0.929	0.934	0.071	0.929	0.0
	302.85	0.952	0.965	0.050	0.950	0.2
300	276.39	0.932	0.937	0.040	0.960	-3.0
	302.85	0.958	0.967	0.030	0.970	-1.2

Table 7: Comparison of experimental and simulated coincidence summing correction factors of ^{133}Ba for Marinelli beaker source.

Volumes (ml)	Energy (keV)	CSF _{Exp}	CSF _{Cal}	$\langle J_1 \rangle \langle J_2 \rangle$	CSF _{Simu}	RD (%)
450	276.39	0.927	0.918	0.086	0.914	1.4
	302.85	0.947	0.958	0.035	0.965	-1.9
600	276.39	0.920	0.923	0.062	0.938	-1.9
	302.85	0.945	0.961	0.050	0.950	-0.5
800	276.39	0.932	0.924	0.064	0.936	-0.4
	302.85	0.957	0.961	0.040	0.960	-0.3
1000	276.39	0.932	0.924	0.066	0.934	-0.2
	302.85	0.958	0.961	0.031	0.969	-1.1

scattered in the samples itself at greater density. This analysis shows that the CSF value increased with the self-absorption of the source matrix.

The proposed simulated method was also applied to obtain the CSF values of ^{133}B and ^{152}Eu . The CSF_{simu} value for ^{133}B (276.39 keV) was calculated using Eq.16 with total efficiency of 160.61 keV. Similarly, CSF_{simu} value was calculated for 302.85 keV

using Eq. 19 with emission probability ratio $\left(\frac{p_1}{p_2}\right)$

of (80.99 keV and 302.85 keV) and total efficiency of 80.99 keV. The simulated values were compared with the experimental results for cylindrical and Marinelli beaker sources as shown in Table 6 and Table 7. The simulated results agreed with the experimental values within 2% for all source volumes, except for the 50 ml and 300 ml where they are up to 3%. In the case of ^{152}Eu , Eq.16 was used to calculate the CSF_{simu} value for (778.9 KeV, 964.0 KeV and 444.0 KeV) with respect to the total efficiency of 344.3 keV, 1085.9 keV and 121.8 keV. The sim-

ulated results were compared with the experimental and calculated CSF values and obtained good agreements with experimental as shown in Table 8 and Table 9.

Conclusions

A new method was used in GEANT4 to calculate the coincidence summing correction factors from the peak and total efficiencies and obtained accurate results for ^{60}Co , ^{88}Y , ^{133}Ba and ^{152}Eu , the average discrepancies between the experimental and simulated results were less than 1%. The simulation was performed and obtained the coincidence summing correction factors for various source volumes and observed the dependence of correction factors value on different samples densities. An easy technique developed in this study for the calculation of coincidence summing correction factor of complex nuclides. The suggested simulation method avoids the preparation of a great variety of gaseous samples with several isotopes and has added the advantages to improve the detection efficiencies for

Table 8: Comparison of experimental and simulated coincidence summing correction factors of ^{152}Eu for cylindrical source.

Volumes (ml)	Energy (keV)	CSF _{Exp}	CSF _{Cal}	$\langle J_1 \rangle$	CSF _{Simu}	RD (%)
50	778.9	0.903	0.906	0.083	0.917	-1.5
	964.0	0.920	0.933	0.065	0.935	-0.2
	444.0	0.902	0.884	0.086	0.914	-3.0
100	778.9	0.894	0.911	0.091	0.909	-1.6
	964.0	0.914	0.935	0.077	0.923	-0.9
	444.0	0.914	0.889	0.083	0.917	-0.3
200	778.9	0.907	0.921	0.078	0.922	-1.6
	964.0	0.925	0.942	0.067	0.933	-0.8
	444.0	0.927	0.901	0.065	0.935	-0.8
300	778.9	0.916	0.924	0.071	0.929	-1.4
	964.0	0.923	0.946	0.073	0.927	-0.4
	444.0	0.932	0.905	0.058	0.942	-1.0

Table 9: Comparison of experimental and simulated coincidence summing correction factors of ^{152}Eu for Marinelli beaker source.

Volumes (ml)	Energy (keV)	CSF _{Exp}	CSF _{Cal}	$\langle J_1 \rangle$	CSF _{Simu}	RD (%)
450	778.9	0.870	0.887	0.111	0.889	-2.0
	964.0	0.894	0.922	0.922	0.912	-2.0
	444.0	0.888	0.859	0.095	0.905	-1.9
600	778.9	0.967	0.893	0.030	0.970	-0.3
	964.0	0.899	0.927	0.085	0.915	-1.7
	444.0	0.894	0.867	0.088	0.912	-2.0
800	778.9	0.870	0.896	0.110	0.890	-2.2
	964.0	0.895	0.929	0.090	0.910	-1.6
	444.0	0.894	0.870	0.095	0.905	-1.2
1000	778.9	0.875	0.897	0.108	0.892	-1.9
	964.0	0.904	0.930	0.087	0.913	-0.9
	444.0	0.908	0.972	0.083	0.917	-0.9

the measurement of the activity of environmental samples.

Acknowledgments

This work at Xian Jiaotong University was fully supported by the Chinese government.

References

1. K Debertin, U Schötzig (1979) Coincidence summing corrections in Ge (Li)-spectrometry at low source-to-detector distances. Nuclear Instruments and Methods 158: 471-477.
2. MI Abbas (2001) HPGe detector photopeak efficiency calculation including self-absorption and coincidence corrections for Marinelli beaker sources using compact analytical expressions. Applied Radiation and Isotopes 54: 761-768.
3. H Jäderström, W Mueller, V Atrashkevich, A Adekola (2015) True coincidence summing correction and mathematical efficiency modeling of a well detector. Nuclear Instruments and Methods in Physics Research Section A: Accelerators, Spectrometers, Detectors and Associated Equipment 784: 264-268.
4. TK Wang, WY Mar, TH Ying, CH Liao, CL Tseng (1995)

- HPGe detector absolute-peak-efficiency calibration by using the ESOLAN program. *Appl Radiat Isot* 46: 933-944.
5. MI Abbas (2007) Direct mathematical method for calculating full-energy peak efficiency and coincidence corrections of HPGe detectors for extended sources. *Nuclear Instruments and Methods in Physics Research Section B: Beam Interactions with Materials and Atoms* 256: 554-557.
 6. E Tomarchio, S Rizzo (2011) Coincidence-summing correction equations in gamma-ray spectrometry with p-type HPGe detectors. *Radiation Physics and Chemistry* 80: 318-323.
 7. M Lee, TS Park, JK Woo (2008) Coincidence summing effects in gamma-ray spectrometry using a Marinelli beaker. *Appl Radiat Isot* 66: 799-803.
 8. MS Badawi, SI Jovanovic, AA Thabet, AM El-Khatib, AD Dlabac, et al. (2017) Calibration of 4π NaI(Tl) detectors with coincidence summing correction using new numerical procedure and ANGLE4 software. *AIP Advances* 7: 035005.
 9. AM El-Khatib, BA Salem, MS Badawi, MM Gouda, AA Thabet, et al. (2017) Full-Energy peak efficiency of an NaI (Tl) detector with coincidence summing correction showing the effect of the source-to-detector distance, *Chinese Journal of Physics* 55: 478-489.
 10. Z Wang, B Kahn, JD Valentine (2002) Efficiency calculation and coincidence summing correction for germanium detectors by Monte Carlo simulation. *IEEE Transactions on Nuclear Science* 49: 1925-1931.
 11. T Vidmar, A Likar (2005) Calculation of total efficiencies of extended samples for HPGe detectors, *Nuclear Instruments and Methods in Physics Research Section A: Accelerators, Spectrometers, Detectors and Associated Equipment* 555: 251-254.
 12. AM Ababneh, MM Eyadeh (2015) Coincidence summing corrections in HPGe gamma-ray spectrometry for Marinelli-beakers geometry using peak to total (P/T) calibration. *Journal of Radiation Research and Applied Sciences* 8: 323-327.
 13. T Vidmar, M Korun, B Vodenik (2007) A method for calculation of true coincidence summing correction factors for extended sources. *Applied radiation and isotopes* 65: 243-246.
 14. D Arnold, O Sima (2004) Application of GESPECOR software for the calculation of coincidence summing effects in special cases. *Applied radiation and isotopes* 60: 167-172.
 15. M Blaauw, SJ Gelsema (2003) Cascade summing in gamma-ray spectrometry in marinelli-beaker geometries: the third efficiency curve. *Nuclear Instruments and Methods in Physics Research Section A: Accelerators, Spectrometers, Detectors and Associated Equipment* 505: 311-315.
 16. S Hurtado, M Garcia-León, R Garcia-Tenorio (2004) GEANT4 code for simulation of a germanium gamma-ray detector and its application to efficiency calibration. *Nucl Instr Meth Phys Res A* 518: 764-774.
 17. B Quintana, C Montes (2014) Summing-coincidence corrections with Geant4 in routine measurements by γ spectrometry of environmental samples. *Applied Radiation and Isotopes* 87: 390-393.
 18. W Khan, Q Zhang, C He, M Saleh, (2018) Monte Carlo simulation of the full energy peak efficiency of an HPGe detector. *Applied Radiation and Isotopes* 131: 67-70.

ISSN 2631-5017



9 772631 501003